

The potential of near-infrared high-resolution studies on the field of galaxies in the young universe

Markus Wittkowski

European Southern Observatory, Casilla 19001, Santiago 19, Chile, mwittkow@eso.org

September 30, 2001

Abstract So far, high resolution techniques on the one hand provide morphological information on bright nearby objects. On the other hand, telescopes with large collecting areas allow us to detect very faint and distant objects, but not to obtain a spatial resolution which is sufficient for detailed morphological studies. Currently, the construction of large optical and infrared interferometers like the Keck Interferometer, the Very Large Telescope Interferometer (VLTI) and the Large Binocular Telescope Interferometer (LBTI) is in progress. These instruments will simultaneously provide larger collecting areas and higher spatial resolutions than current instruments. Thus, they might enable for the first time near-infrared studies of galaxies in the young universe with an absolute spatial resolution as available today only for the closest galaxies. Using recent results in the field of high resolution studies of nearby galaxies, a rough idea of what might be expected to be observed is given. The concepts of the forthcoming interferometers is reviewed and technical aspects that are essential for observations of distant galactic centers are discussed. An outlook is given on which observational tasks can be addressed to these instruments and how the results will increase our knowledge in the field of the evolution of galaxies and the universe.

1 Introduction

”For all cosmic objects, we would ideally like to know the flux density over the entire electromagnetic spectrum. This goal is now almost achieved, at least for the brightest objects in each important class. The obvious next goal is to map out each object’s structure in as much detail as possible.”

Martin R. Rees (2000)

As nicely expressed by Martin R. Rees (2000), high-resolution studies directly revealing the morphology of astrophysical objects are an essential tool to further our understanding of all parts of astrophysics, and have so far often been the key to milestone achievements. While studies with highest resolutions down to the order of 1 mas using interferometric techniques became already routine tools at radio wavelengths with facilities like the VLBI (Very Large Baseline Interferometer), large optical and infrared interferometers are in the process of being constructed right now. Several optical and infrared interferometric instruments with relatively small collecting areas have been operated starting with the pioneer works by Fizeau (1868, 1873) and Michelson (1890)¹. The first construction of large interferometric facilities with 8-10 m class telescopes and baselines up to the order of 100 m is currently in progress with the Keck, VLTI (Very Large Telescope Interferometer), and LBT (Large Binocular Telescope) interferometers. First fringes at the Keck interferometer were achieved in February 2001 using test siderostats and in March 2001 using the two 10 m telescopes (JPL News Release from March 14, 2001). First fringes at the VLTI using test siderostats followed closely in March 2001 (ESO Press Release 06/01 from March 18, 2001) and the first beam combination using the 8 m unit telescopes is envisioned for November 2001. The LBT will provide a complimentary

¹An excellent overview on past and present optical long-baseline interferometry is provided by Peter Lawson at “ol-bin.jpl.nasa.gov”.

interferometric facility with two 8.4 m telescopes on one mount from about 2004. Further interferometric beam combinations as those between the Subaru telescope and a neighbor have been discussed (Nishikawa et al. 1998). These facilities with their large collecting areas will be the first instruments that allow us to study galactic centers with spatial resolutions down to the order of 1 mas at optical and infrared wavelengths. With the 120 m VLTI baseline the resolution λ/B at $1.2 \mu\text{m}$ is 2 mas, i.e. about the same as currently achieved at radio wavelengths with VLBI. This angular resolution will allow us to study close galactic centers at optical and infrared wavelengths with there unprecedented absolute spatial resolution, as well as distant galactic centers with absolute spatial resolutions as available today for only the closest galaxies. The feasibility of the latter is discussed in this article. Previous publications mentioning optical interferometric observations of high-redshift objects include Voit (1997), Tytler (1997), and Angel et al. (1998). In Sect. 2 general principles of interferometry are briefly reviewed and their implications on the feasibility of this project are discussed, followed by a review of the concepts of the actual interferometers and instruments. The center of the Seyfert galaxy NGC 1068 is one of the best studied nearby active galactic nuclei (AGN). High-resolution studies of this object at the diffraction-limit of current single telescopes are reviewed in Sect.3 in order to provide a first rough idea of the structures that can be expected to be observed in the case of high-redshift galactic centers. This object is then put to different redshifts, and observational limits by apparent magnitude and spatial resolution are analyzed. Finally, in Sect. 4, these results are summarized and additional issues are mentioned, as further scientific objectives and observational prospects in the more distant future. The latter include the use of extremely large telescopes (ELT) with diameters of the order of 100 m. Several concept studies of such projects have been started, for instance the 100 m "OWL" (for *Overwhelmingly Large Telescope*) project (see Dierickx & Gilmozzi 2000 for the conceptual design and Gilmozzi 2000 for science opportunities).

2 Interferometry

Until extremely large optical telescopes with diameters of the order of 100 m become available, optical and infrared studies with spatial resolution down to about 1 mas require the use of interferometers. Interferometric measurements record the amplitude and phase of interference fringes rather than directly providing images. The basic implications of this technique on the feasibility of our project is discussed in the following. The characteristics of the different interferometers and their instruments is given at the end of this section.

Field of view Two types of interferometry have to be distinguished, namely the image plane or "Fizeau" and the pupil plane or "Michelson" beam combinations². The former technique implies that the output pupil equals the input pupil or a scaled version of it for the whole integration time, so that the beams can interfere at the final (output) image plane. This configuration can most easily be achieved if all apertures share one mount, and the entrance pupil is constant for all pointing directions. Then, the field of view is limited only by the performance of the optical components, e.g. the adaptive optics system. Such a configuration was chosen in the case of the LBT interferometer, and, at near-infrared wavelengths, a field of view of one arcmin or more is expected (Herbst et al. 2000). The pupil plane or "Michelson" beam combination technique, as chosen for the Keck and VLT interferometers, a configuration where input and output pupils are not equal, limits the field of view to about 1 arcsec. It has the advantage of allowing long baselines. With this technique, spatial filtering is often applied in order to improve the accuracy of the measured visibility values, which further limits the field of view

²The terms image plane and Fizeau beam combination, as well as pupil plane and Michelson beam combination are sometimes not used synonymously. In fact, it is in principle possible to achieve an image plane beam combination with a Michelson style interferometer, as mentioned later in this article

Table 1: Cross correlation of high-redshift ($z \geq 0.5$) objects in the catalog "Quasars and Active Galactic Nuclei (8th Ed.)(Veron-Cetti & Veron 1998)" with objects in the HIPPARCOS catalog (Perryman & ESO 1997) with a distance of up to 1 arcmin. The table lists the name of the AGN, its redshift z , its apparent V magnitude V_{AGN} , its bolometric luminosity M_{bol} , the distance to the HIPPARCOS star d , the HIPPARCOS catalog number HIP, the star's spectral type Sp.T., and its apparent V magnitude V_{Ref} .

AGN	z	V_{AGN}	M_{bol}	d [arcsec]	HIP	Sp.T.	V_{Ref}
B19.09	2.02	18.2	-27.8	58.9	9296	G8III	6.9
PKS 0435-300	1.33	17.5	-27.4	29.2	21550	F5V	8.1
OK 568	0.57	18.6	-24.1	28.3	47818	K0	8.7
AH 26	2.21	18.6	-27.5	20.3	64269	K0III	8.4
PKS 1551+130	1.29	17.7	-26.8	54.8	77830	F0	11.4

to the size of one airy disk. This field of view will usually be sufficient, since the interest concerns scales which are not available with single telescopes at their diffraction limit. Admittedly, for objects which are themselves not bright enough to allow for adaptive optics and fringe tracking, as those discussed in this article, a limited field of view decreases the probability to find a bright reference star within this field. To cope with this, Michelson style interferometers can be equipped with a so called "dual feed facility" which allows us to feed two fields into the beam combiner. The second field can then be chosen to include the reference star. The maximum separation of the two fields is again limited by the optical quality and, for the example of the VLTI, amounts to about 1 arcmin, which equals the field of view of Fizeau type interferometers.

Magnitude limit The incoming wavefront above each aperture is corrupted by atmospheric phase noise. Hence, each beam has to be corrected for this effect using the technique of adaptive optics before the beams are combined. This requires that the wavefront has to be analysed on sub-apertures with the size of the Fried parameter r_0 , limiting the magnitude of the reference star. Despite this correction, the optical path difference between two telescopes varies due to different mean phase values. Hence, the fringes have to be tracked, which limits the magnitude as well. Either the object itself or a nearby reference star within the isoplanatic patch and the field of view has to be bright enough to allow for adaptive optics and fringe tracking. The critical value is about 12 mag at $2.2 \mu\text{m}$ for the planned interferometers. Since the objects in discussion are generally fainter than this, the use of a reference star for fringe tracking and adaptive optics will be mandatory. Table 1 lists all objects given in the catalog *Quasars and Active Galactic Nuclei (8th Ed.)* (Veron-Cetti & Veron 1998) with a redshift z of larger than 0.5 that have a star given in the HIPPARCOS catalog (Perryman & ESA 1997) within a distance of less than 1 arcmin. Assuming that a field of view of 1 arcmin can be reached, or that a dual feed technique is available (see above), this tests whether such reference stars can be found for the objects in question. A total of 5 AGN/reference star pairs were found. Considering that the Veron catalog is not complete and that the HIPPARCOS catalog is complete only up to a V magnitude of 9, while reference stars up to K magnitude 12, i.e. $V > 12$, can be used, this shows that a sufficient number of AGN with such a reference star will be available.

Imaging capabilities Interferometers measure the amplitude and phase of interference fringes. In absence of atmospheric and instrumental phase noise, this is the amplitude and phase of the complex object visibility, i.e. the fourier transform of the object intensity distribution at a spatial frequency corresponding to the length and orientation of the used baseline. In presence of phase noise, however, an incoherent average of the measured complex visibility values would be caused to zero. The use

Table 2: Overview on first generation interferometric instruments for the Keck, VLT, and LBT interferometers. Given is the name of the interferometer with its maximum baseline; and the name of the instrument with the operating wavelength, the limiting magnitude and the approximate date of first fringes. For further information and references see the text.

Interferometer	max. basel.	Instrument	λ [μm]	lim. magn.	first fringes
Keck	85 m	two-way	1.5-2.5		
		multi-way	1.5-5		
		nulling	10		
VLTI	130 m	AMBER	1-2.5	K \sim 12/20	2003
		MIDI	10-20	N \sim 3/8	2002
		PRIMA			2004
LBTI	23 m	LINC	1-2.4	K \sim 20-26	2004

of a fringe tracker can stabilize the fringe position, but not to an extent that the single phases could be used for imaging. A way to directly derive the fringe phase with sufficient accuracy is the method of "phase referenced imaging". This technique requires a dual feed facility in combination with a metrology system. Then, the differential delay between the fringe positions of a bright reference star and of the faint object is measured, whereas the bright star fringe phase serves as a reference for the object fringe phase. However, this technique is technically difficult to realize. Generally, unbiased estimators exist for the squared visibility amplitudes and for the closure phases, the phase of the triple product or bispectrum, the product of three complex visibilities corresponding to baselines that form a triangle. The object visibility amplitude can then be derived as the square root of the squared visibility amplitude, despite the need of attention to the asymmetric error bars and observed squared visibility values that may have negative values due to noise. In case that measurements were done at all spatial frequencies between zero and a maximum baseline, and with all orientations, the phases of the complex object visibility can be derived by recursion methods. This full " uv -coverage", can be achieved with a configuration like that of the LBT interferometer. Once all complex object visibility values have been recovered, the object intensity distribution can be obtained by fourier-re-transformation. If the uv -coverage is not complete, the object intensity distribution can be reconstructed using imaging techniques which effectively interpolate this limited uv -coverage, as applied in radio interferometry. The signal-to-noise ratio of the final image decreases with decreasing uv -coverage. It decreases as well with increasing number of resolution elements, i.e. with the complexity of the observed object. Hence, the imaging of complex source structures, as might be expected for extended galaxies might turn out to be impossible with interferometers that provide only a limited uv -coverage, as the VLTI or Keck interferometer. Here, imaging or model fits that determine only a few basic parameters of the compact central cores might be a better choice. In the context of high-redshift galactic centers, such simple compact structures could be the expected dust tori, the inner parts of jets, or structures between broad line and narrow line region. A more detailed discussion of the structures that might be expected follows in section 3.

Available interferometers and their instruments Interferometers in construction that will provide collecting areas large enough to allow observations of galactic centers include the Keck, VLTI, and LBT interferometers. The Keck interferometer is located on Mauna Kea, Hawaii, the VLTI on Cerro Paranal, Chile, and the LBT on Mt. Graham, Arizona. The Keck and VLT interferometers are "Michelson" style (see above) facilities and provide relatively large maximum baselines of 85 m and 130 m, respectively. As a result, the available uv -coverage (see above) is not complete, and the field of view is limited to about 1-2 arcsec. However, "dual feed facilities" (see above) are planned,

that allow the use of a bright reference star for adaptive optics and fringe tracking. Planned Keck instruments include near-infrared two-way combiners for astrometry, two-element fringe tracking, and co-phasing; a near-infrared multi-way imaging combiner; and a mid-infrared nulling combiner (Colavita & Wizinowich 2000). First VLTI instruments include the mid-infrared instrument MIDI and the near-infrared instrument AMBER, followed by the dual feed facility PRIMA (Glindemann et al. 2000). AMBER will allow the combination of three beams, and thus will provide imaging capabilities. Using PRIMA to provide a bright ($K \sim 12$) reference star, AMBER will have a limiting K magnitude of about 20, and MIDI a limiting N magnitude of about 8. PRIMA can also be used for phase referenced imaging (see above), allowing imaging with both MIDI and AMBER, for fainter objects than with closure phase techniques (Delplancke et al. 2000). The LBT interferometer is a "Fizeau" style facility with two 8.4 m telescopes on one mount. This facility will provide a fairly complete uv -coverage and a relatively large field of view of 1 arcmin, on the cost of a more limited spatial resolution corresponding to a maximum baseline of 23 m. An interferometric beam combiner, LINC, is planned as one of the first light instruments. It will operate at wavelengths from $1 \mu\text{m}$ to $2.4 \mu\text{m}$ with a limiting K magnitude of 26.3 for a point source detection and 19.6 for the reconstruction of extended sources, under certain assumptions (Herbst et al. 2000). Table 2 gives an overview of the planned VLTI and LBTI instruments of the first generation. While a nulling beam combiner, which can exclude the light from the central point source, is planned as a first generation instrument at the Keck interferometer, such an instrument is in discussion as a second generation instrument for the VLTI. Further discussions on future instruments include homothetic pupil mapping for Michelson style interferometers, fiber optics with coherent amplifiers to send the light to the beam combination lab, and artificial guide stars for fringe tracking.

3 Expected structures and observational limits

The Seyfert Galaxy NGC 1068 as a prototype galactic center The Seyfert galaxy NGC 1068 harbors one of the brightest and closest active galactic nuclei (AGN). Hence, it is one of the best studied galactic centers and observations of this object, combined with theoretical modeling like radiation transfer calculations, have substantially contributed to our current view on the structure of AGN. In fact, it is one of the objects studied in the classical work by Seyfert (1943) and it is the archetype of type 2 Seyfert galaxies. The observation by Antonucci & Miller (1985) exhibiting broad emission lines in polarized light, initiated the unification scheme for AGN (see Antonucci 1993 for a recent review). In particular, high-resolution studies of this object have been performed at a wide range of wavelengths, testing and extending our view on the unification scheme. In this article, high-resolution information on NGC 1068 is used to provide an idea on which structures might be expected to be observed in the case of more distant galactic centers with higher angular resolution, i.e. with the same absolute spatial resolution as available today for NGC 1068. HST observations with an angular resolution of ~ 0.1 arcsec were obtained at the UV continuum, the optical continuum and the [OIII] 501 nm emission line (Macchetto et al. 1994). These images show the narrow-line region, a conus-shaped structure, with the central source being obscured. Radio observations with similar angular resolution were performed by Ulvestad et al. (1987), Gallimore et al. (1996a,b), Muxlow et al. (1996). These observations show several radio peaks in approximately NE-SW direction, of which only one ("S2") shows a positive spectral index α ($S_\nu \sim \nu^\alpha$), and is considered the position of the central core. The other emission peaks are connected with the radio jet. The central source S2 was studied by Gallimore et al. (1997) at 8.4 GHz with a very high angular resolution of ~ 1 mas, revealing a structure approximately perpendicular to the radio jet, which is interpreted as emission from the torus surrounding the central nucleus. Mid-infrared observations were carried out by Chelli et al. (1987), Bock et al. (1998), Marco & Alloin (1999), Alloin et al. (2000), Bock et al. (2000), showing a

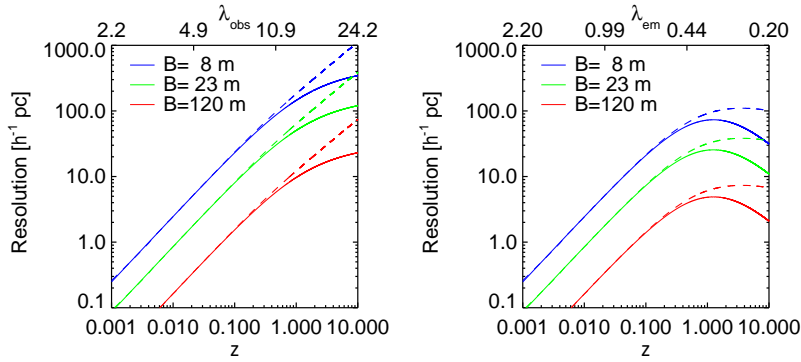


Figure 1: Absolute spatial resolution based on Einstein-de-Sitter ($\Omega_M=1$, solid line) and low density ($\Omega_M=0.05$, dashed line) world models. Left: Flux emitted at $\lambda_{em}=2.2 \mu\text{m}$; Right: Observing wavelength: $\lambda_{obs}=2.2 \mu\text{m}$. For the angular resolution, $0.3 \lambda/B$ was used, corresponding to a decrease of the squared visibility to 80%.

compact central core, extended emission in approximately N-S direction on short scales and structures corresponding to the radio peaks on larger scales. Marco & Alloin (1999) report an additional 80 pc E-W structure along the position angle of the 8.4 GHz radio continuum image, interpreted as the torus at mid-infrared wavelengths. Near-infrared studies by McCarthy et al. (1982), Thatte et al. (1997), Rouan et al. (1998), and Weinberger et al. (1999) confirm a very compact central NIR core and extended emission in N-S direction with a size of the order of 10 pc. The central $2.2 \mu\text{m}$ core was resolved by bispectrum speckle interferometry at the diffraction-limit of the Russian 6 m telescope, with a FWHM size of $\sim 30 \text{ mas}$ or $\sim 2 \text{ pc}$ for an assumed Gaussian intensity distribution and a flux of $F_K^{30 \text{ mas}} = 520 \text{ mJy} \pm 210 \text{ mJy}$ (Wittkowski et al. 1998). With a model of an unresolved source contributing 50% to the flux of the 30 mas component (the maximum percentage consistent with the obtained visibility function), this compact component had a size of $\sim 45 \text{ mas}$ instead of 30 mas, i.e. still being a very compact source with a size of a few parsec. More recent speckle observations seem to indicate that this compact core is asymmetric with a position angle of $\sim 20^\circ$, and an additional more extended structure in N-S direction out to $\sim 25 \text{ pc}$ (Wittkowski et al. 1999), consistent with other NIR observations mentioned above. An interpretation for the very compact 30-45 mas structure could be a dust component, e.g. at the wall of the conus, very close to the central source, scattering and emitting near-infrared light; possibly with an additional component of direct light from the central source. The more extended $\sim 200 \text{ mas}$ structure might be central light scattered at electrons and dust further out in the ionization cone. The interferometers as described above work at near-infrared and mid-infrared wavelengths, and might only be able to map very compact sources, due to the signal-to noise ratio after image processing. Thus, these very compact near-infrared structures with sizes of 2-4 pc and the slightly more extended structures out to tens of parsec, connected to the torus, the region between NLR and BLR, or the inner part of the jet, are most promising structures to be observed with these interferometers at more distant galactic centers. These measurements could then initiate extensions of our view on the structures at the very centers of AGN as a function of the universe's age. In the following paragraphs, the observational limits are discussed, when observing these NGC 1068-like structures at higher redshifts. It should be kept in mind, however, that this is only a rough idea of what might be expected to be observed and that actual structures might be different.

Observation of a NGC 1068-like object at different redshifts. Here, limits for the study of structures like those observed at near-infrared wavelengths for NGC 1068, but for different redshifts, are derived based on the spatial resolution and the flux. Figure 3 shows the absolute spatial resolution that can be achieved with baselines of 8 m (single VLT UT telescopes), 23 m (LBT), and 120 m (VLTI) as a function of redshift. Shown are two cases, where (1) light emitted at $2.2 \mu\text{m}$ is observed, and (2) the object is observed at $2.2 \mu\text{m}$. The former case regards to the near-infrared structures observed at NGC 1068, which would be shifted to longer wavelengths. The latter case gives higher spatial resolution but it is less clear whether there are structures feasible to observe since light emitted at shorter

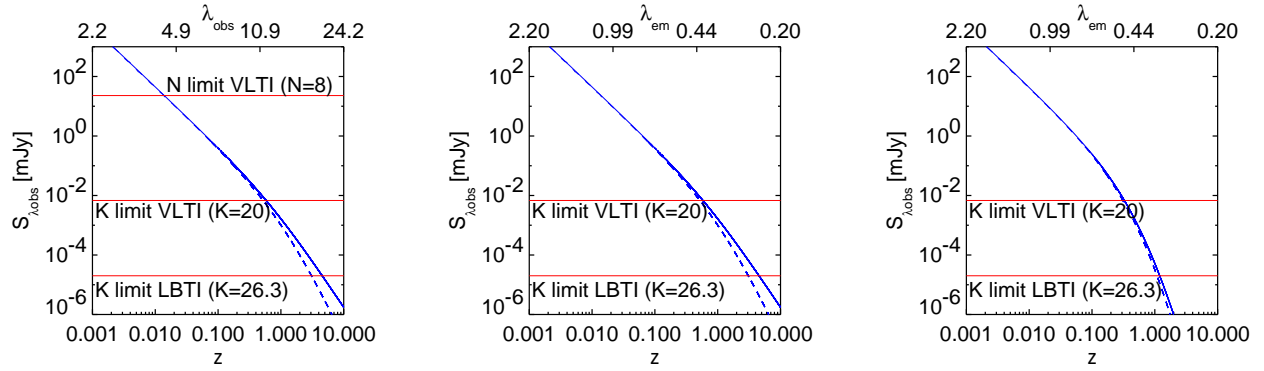


Figure 2: Flux of a source with $F_K(z = 0.003) = 500$ mJy (compact K-band component of NGC 1068) as a function of redshift. Left: Flux is emitted at $\lambda_{\text{em}} = 2.2 \mu\text{m}$; Middle and right: Observing wavelength is $\lambda_{\text{obs}} = 2.2 \mu\text{m}$, whereas (middle) is based on the assumption of a constant source spectrum, and (right) on that of a Planck source spectrum with $T = 1500$ K. As in Fig. 3, the solid lines denote a Einstein-de-Sitter world model and the dashed lines a low density world model.

Table 3: Observational limits for the redshift z . Left: Limit by spatial resolution. Right: Limit by magnitude assuming a source flux of 0.5 Jy at $2.2 \mu\text{m}$ for $z = 0.003$.

Structure	8 m	23 m	120 m	for $z = 1$		
2 pc, $\lambda_{\text{em}} = 2.2 \mu\text{m}$	0.008	0.025	0.15	5 km		
20 pc, $\lambda_{\text{em}} = 2.2 \mu\text{m}$	0.08	0.25	2-6	90 m	$\lambda_{\text{em}} = 2.2 \mu\text{m}$	0.05
					$\lambda_{\text{obs}} = 2.2 \mu\text{m}$	const.
					$\lambda_{\text{obs}} = 2.2 \mu\text{m}$	0.3-1
2 pc, $\lambda_{\text{obs}} = 2.2 \mu\text{m}$	0.008	0.025	0.15	3 km		Planck
20 pc, $\lambda_{\text{obs}} = 2.2 \mu\text{m}$	0.1	0.4	–	50 m		

wavelengths is studied, where the central source might be completely obscured. These graphs were obtained using the angular diameter distance given by Hogg (2000). Figure 2 shows analogously the observable flux of a source with 500 mJy at $2.2 \mu\text{m}$ for $z = 0.003$ (compact NGC 1068 structure) as a function of redshift, based on the luminosity distance given by Hogg (2000). The magnitude limits of the interferometers discussed above are shown. For $2.2 \mu\text{m}$ as the observing wavelength, an assumption on the source spectrum has to be made. Shown are the results for a constant source spectrum – a good model for direct or scattered light originating from the central continuum source – and for a Planck spectrum with $T=1500 \text{ K}$ – a model for thermal radiation from dust components. Table 3 shows the resulting observational constraints by spatial resolution and magnitude. It should be noted that the spatial resolution limit is a hard limit, whereas the magnitude limit might be more favorable since high-redshift objects are likely to have a higher intrinsic luminosity than NGC 1068. Table 4 shows that objects with large bolometric luminosity are likely to be found at high redshifts. Objects with a bolometric luminosity larger than that of NGC 1068 by a factor of 10^4 can be found. Observations of the compact 2 pc structure are limited by spatial resolution to about $z = 0.15$. The limit by magnitude based on the assumption of the NGC 1068 magnitude is about $z = 0.05$ considering structures emitting at $2.2 \mu\text{m}$, and there is almost no flux limit for structures observed at $2.2 \mu\text{m}$. In order to observe such a compact structure emitting at $2.2 \mu\text{m}$ out to $z = 1$, an interferometer consisting of 400 m diameter mirrors and baselines of 3-5 km would be needed. The observation of a 20 pc NGC 1068 structure in the young universe is not limited by spatial resolution, but only by magnitude, which is $z = 0.05$ for an emitting wavelengths of $2.2 \mu\text{m}$, and $z = 1 - 4$ for an observing wavelength of $2.2 \mu\text{m}$. Again, much brighter objects are likely to be available, though.

Table 4: Bolometric flux of NGC 1068 in comparison to all AGN in Veron & Veron (1998) with $M_{\text{bol}} \leq -29$. It turns out that objects with highest bolometric luminosity are likely to be found at high redshifts.

Name	z	V	M_{bol}	Name	z	V	M_{bol}
NGC 1068	0.003	10.8	-19.6	0846+51W1	1.9	15.7	-29.4
Q 0042-2627	3.3	17.7	-29.6	PG 1718+481	1.1	14.6	-29.8
DHM 0054-284	3.6	18.2	-29.3	PKS 2000-330	3.8	17.3	-30.0
Q 0130-403	3.0	17.0	-30.0	Q 2204-408	3.2	17.6	-29.1
Q 0324-407	3.1	17.8	-29.9				

4 Summary and discussion

The feasibility of observing galactic centers in the young universe at infrared wavelengths with very high angular resolution of up to about 1 mas has been studied. Interferometers in construction that might allow such measurements for the first time have been discussed. Observations of the nearby AGN NGC 1068 with the same absolute spatial resolution as intended here for high-redshift objects, have been reviewed to give an idea of the structures that might be expected to be observed. These structures include a compact near-infrared core with a size of 2-4 pc and a K-band flux of 0.5 Jy, and extended emission out to tens of parsecs. These components might be connected to the torus, the region between BLR and NLR, and the inner part of the radio jet. Using these NGC 1068 structures as a prototype, the observational limits by spatial resolution and magnitude for such structures at high-redshift were derived. Such measurements might aim at testing and extending our unification scheme of galactic centers including an evolution with the universe's age. Results are given in Table 3. However, the assumption of NGC 1068-like structures is considered only a starting point for these studies, and, of course, structures might differ for high-redshift object. For example, it was shown that high-redshift objects with much higher intrinsic luminosity are likely to be found. This may also lead to different length-scales of typical structures. Furthermore, there seem to be more type I objects in the young universe than today, which might complicate observations of structures which are relatively faint compared to less obscured central objects. There are also further scientific objectives that have not been discussed in detail, but an estimate of their feasibility might be supported by the discussions and figures given above as well. These objectives include observations of deep fields and of host galaxies using instruments with a fairly complete uv -coverage and large field of view like the LBT, with unprecedented spatial resolution. Another objective is the measurement of motions and parallaxes of galactic centers using phase reference techniques. If structures as discussed above are found, a further step in the more distant future could be the recording of spectra to derive velocity information and to determine black hole masses as a function of redshift. Such scientific objectives might be supported by even more advanced instrumental options in the more distant future. In the field of interferometry, these second-generation instrumentation might include beam combinations with fiber optics and coherent amplifications to obtain a better magnitude limit. A larger number of feasible objects could become available by using artificial guide stars for adaptive optics and fringe tracking. An enlarged field of view for Michelson style interferometers might be reached by homothetic mapping. Nulling interferometric instruments, which cancel out the light of the central source and image only off-center structures, might help to observe faint structures close to not-obscured central sources. Polarimetric interferometric observations might become available which would be of great value since the origin of observed structures could be investigated in more detail, i.e. whether structures are composed of reflected light, direct emission from the central source, or thermal emission. Finally, observations of these objects will become much easier with the construction of extremely large telescopes with diameters of up to 100 m, like the OWL telescope (see Sect. 1). In an even

further step one might think of interferometers with baselines on km scales consisting of OWL telescopes, which was for instance mentioned by Glindemann et al. (2001) and called the "la OLA" project (for *Overwhelmingly Large Array*). Such an instrument would enable us to observe the compact NGC 1068 2-4 pc component, emitted at near-infrared and observed at mid-infrared wavelengths, out to a redshift of $z = 1$.

Acknowledgements I thank Sara Ellison, Andreas Glindemann and Markus Schöller for information, help, and discussions during the preparation of this talk. I acknowledge previous discussions on related aspects with members of the "MPIfR Infrared Interferometry" and NPOI groups.

References

- Alloin D., Pantin E., Lagage P.O., Granato G.L., 2000, A&A 363, 926
Angel J.R.P., Hill J.M., Strittmatter P.A., Salinari P, Weigelt G., 1998, SPIE 3350, 881
Antonucci R.R.J., Miller J.S., 1985, ApJ 297, 621
Antonucci R., 1993, ARAA 31, 473
Bock J.J., Marsh K.A., Ressler M.E., Werner M.W., 1998, ApJ 504, L5
Bock J.J., Neugebauer G., Matthews K., Soifer B.T., Becklin E.E., Ressler M., Marsh K., Werner M.W., Egami E., Blandford R., 2000, AJ 120, 2904
Chelli A., Perrier C., Cruz-Gonzalez I., Carrasco L., 1987, A&A 177, 51
Delplancke F., Leveque S., Kervella P., Glindemann A., d'Arcio L., 2000, SPIE 4006, 365
Dierickx P., Gilmozzi R., 2000, SPIE 4004, 290
Fizeau A.H., 1868, CRAS 66, 934
Fizeau A.H., 1873, CRAS 76, 1008
Gallimore J.F., Baum S.A., O'Dea C.P., Pedlar A., 1996a, ApJ 458, 136
Gallimore J.F., Baum S.A., O'Dea C.P., 1996b, ApJ 464, 198
Gallimore J.F., Baum S.A., O'Dea C.P., 1997, Nature 388, 852
Gilmozzi R., 2000, SPIE 4005,
Glindemann A., et al., 2001, in Scientific Drivers for ESO Future VLT/VLTI Instrumentation, Garching 11-15 June 2001, eds. J. Bergeron, G. Monnet
Herbst T.M., Rix H.-W., Bizenberger P., Ollivier M., 2000, SPIE 4006, 673
Hogg, D. W., 2000, astro-ph/9905116v4
Macchetto F., Capetti A., Sparks W.B., Axon D.J., Boksenberg A., 1994, ApJ 435, L15
Marco O., Alloin D., 2000, A&A 353, 465
McCarthy D.W., Low F.J., Kleinmann S.G., Gillet F.C., 1982, ApJ 257, L7
Michelson A.A, 1890, The London Edingburgh and Dublin Philosophical Magazine and Journal of Science, Ser. 5, Vol. 30, No. 182, p. 1-21
Nishikawa J., Sato K., Fukushima T., Yoshizawa M., Machida Y., Honma Y., 1998, SPIE 3350, 184
Perryman M.A.C and ESA, 1997, The HIPPARCOS and TYCHO catalogues, ESA SP Series vol. 1200, Noordwijk, Netherlands: ESA Publication Division
Rees M. J., 2000, IAUS 205, 1
Rouan D., Rigaut F., Alloin D., Doyon R., Lai O., Crampton D., Gendron E., Arsenault R., 1998, A&A 339, 687
Seyfert C.K., 1943, ApJ 97, 28
Tytler D., 1997, in Science with the VLT Interferometer, Springer 1997, p. 121
Ulvestad J.S., Neff S.G., Wilson A.S., 1987, AJ 92, 22
Veron-Cetti M.P., Veron P., 1998, ESO Scientific Report 18
Voit G.M., 1997, in Science with the VLT Interferometer, Springer 1997, p. 104
Weinberger A.J., Neugebauer G., Matthews K., 1999, AJ 17, 2748
Wittkowski M., Balega Y., Beckert T., Duschl W.J., Hofmann K.-H., Weigelt, G., 1998, A&A 329, L45
Wittkowski M., Balega Y., Hofmann K.-H., Weigelt G., 1999, AGM 15, 83